Journal of Applied Physics PERSPECTIVE scitation.org/journal/jap

Current perspective in magnetocaloric materials research

Cite as: J. Appl. Phys. **133**, 040903 (2023); doi: 10.1063/5.0130035
Submitted: 8 October 2022 · Accepted: 4 January 2023 ·
Published Online: 27 January 2023

Jia Yan Law,[a] Luis M. Moreno-Ramírez, Álvaro Díaz-García, and Victorino Franco[a]

AFFILIATIONS

Dpto. Física de la Materia Condensada, ICMS-CSIC, Universidad de Sevilla, P.O. Box 1065, 41080 Sevilla, Spain

[a]**Authors to whom correspondence should be addressed:** jylaw@us.es and vfranco@us.es

ABSTRACT

Magnetocaloric refrigeration has remained a promising alternative to conventional refrigeration for the last few decades. The delay in reaching the market is significantly based on materials' related issues, such as hysteresis/reversibility, mechanical stability, or formability. This perspective paper shows the current trends in magnetocaloric materials research, highlighting the families of alloys and compounds that are gaining attention in the recent years. It also includes an overview of novel approaches that can be used to analyze these properties that could improve the applicability of magnetocaloric materials.

I. INTRODUCTION

With climate change, people are more dependent on temperature control. Therefore, the increasing electricity consumption and energy efficiency of cooling systems a more of a significant concern today.[1–3] Since the early days of cooling technologies, domestic refrigerators have relied on gas expansion/compression. Although these systems cover a desirable range of temperatures, they are generally energy inefficient (due to compressor loss) and use hazardous chemicals, such as chlorofluorocarbons, liquefied ammonia, or hydrochlorofluorocarbons.[4]

An emerging cooling technology that can double the efficiency of conventional gas-compression refrigerators has been developed. This technology is known as magnetic refrigeration (MR).[5–8] It is based on the magnetocaloric effect (MCE), which describes the reversible temperature change of a magnetic material when adiabatically subjected to a varying magnetic field.[9] Thus, the magnetocaloric material acts as a solid refrigerant in a MR device, eliminating the need for hazardous and ozone-depleting gas refrigerants used in traditional refrigeration systems. Furthermore, without the need for a compressor, MR offers less noise as well as better efficiency than gas-compression refrigeration systems, suggesting that MR and magnetocalorics could address some of the worldwide energy concerns today. The magnetocaloric effect is associated with first-order (FOMT) and second-order (SOMT) thermomagnetic phase transitions.[10,11] For the latter, Gd remains the benchmark material for room temperature applications due to its large magnetic moment. Materials with FOMT typically possess a larger MCE, also termed as giant MCE (GMCE) in the literature. Their magnitudes can be twice as large as that of Gd as reported in $Gd_5Si_2Ge_2$ by V. K. Pecharsky and K. A. Gschneidner, Jr.[12] in 1997. However, the use of these GMCE magnitudes is constrained by the hysteretic behavior of FOMT unlike the fully reversible response of SOMT.[13] Until now, device commercialization has been stymied by several impediments, the most significant of which has been the inability to identify an appropriate magnetocaloric material based on abundant elements with optimized cyclic performance.[14]

In this perspective paper, we discuss the trends in magnetocaloric materials and the open questions about their performance. It also includes proposed hypotheses for their resolution as well as newly implemented methods pertinent to material and performance analysis. Recent comprehensive reviews of magnetocalorics have been covered in Refs. 5, 6, and 15 for materials, Ref. 16 for magnetocaloric composites, Refs. 17 and 18 on magnetocaloric high-entropy alloys, Refs. 19–21 for the characterization protocols for MCE determination, and Ref. 22 on device development.

II. MAGNETOCALORIC MATERIALS NOWADAYS

Since the discovery of GMCE in $Gd_5Si_2Ge_2$, the search for magnetocaloric materials has primarily focused on FOMT materials. However, there are still ongoing efforts for SOMT materials due to their non-hysteretic advantage and effective performance at

low temperatures. Figure 1 displays an infographic based on a literature survey from the Web of Science (WoS) that shows the top families of magnetocaloric materials that have been published recently. The popularity is shown by the percentage of their annual publications from 2019 to 2022 (and the size of the symbol). The symbol colors also indicate an increasing or decreasing trend for the publications: blue for a declining sector, red for a rising sector, and yellowish (with a dashed outline) for constant. It can be seen that the most popular ones are the Ni_2–Mn-X-based Heusler alloys (H·A·s) (especially for X = In or Sn), MM'X, and $La(Fe,Si)_{13}$ alloys, though their first works were reported several years ago.[23–25] The community is still drawn to these materials because of their promising magnetocaloric responses using chemical compositions based primarily on abundant elements. Among them, MM'X-type alloys (e.g., MnCoGe- and MnNiSi-based), in particular, exhibit huge hysteresis in addition to their large caloric effects, implying a need to minimize the former without compensating for overall performance.[26] Many of the recent works on the $La(Fe,Si)_{13}$ family focus on performance optimization through hysteresis tuning and mechanical stability, which has been a concern for high-performing magnetocaloric materials.[27,28] This is followed by the magnetocaloric composites system, which combines multiple magnetocaloric phases or compositions, and was recently extended to address mechanical stability or for H_2 or N_2 liquefaction. Magnetocaloric composites stem from the aim to expand the temperature span of the regenerator (with appropriate phase selection and transition temperatures[16]) since their experimental validation in 1987.[29,30] Furthermore, RE-based intermetallics (restricted to SOMT in this category) attract the community-wide research attention despite their criticality because their MCE was typically found at relatively low transition temperatures in addition to the large intrinsic magnetic moments exhibited in RE elements.[31–34] The next on the list are transition-metal (TM)- and RE-based amorphous alloys, Ni_2MnGa, and high-entropy alloys (HEAs). In spite of ongoing studies on the magnetocaloric behavior of amorphous alloys (SOMT) and Ni_2MnGa H·A·s, they are in the declining sector (blue in color). HEAs, on the other hand, are growing in popularity, primarily because they are still regarded as a new class of materials and have been found to exhibit excellent mechanical properties.[35,36] These alloys are not based on any elements or components as they concentrate on the central region of the multiprincipal elements phase diagram. This is dissimilar to conventional alloys, which are designed by diluting the main constituent with trace elements. The HEA name originated from their high configurational entropy of mixing, and they are well-known for their superior mechanical properties compared to conventional alloys. This design concept encompasses a vast compositional space, which can aid in the discovery of novel alloy compositions and properties. Next in line are the Mn–Fe–P–Si (also generally labeled as Fe_2P), Laves phases ($RETM_2$ stoichiometry), and all-*d*-metal Ni–Co–Mn–Ti families. The well-known performance of Fe_2P continues to draw researchers' interest, with recent efforts focused on optimizing their hysteresis, annealing process, etc.[37–43] However, its significance is diminished due to the persistence of unsought multiphase in the Fe_2P family. In contrast, all *d*-metal Ni–Co–Mn–Ti H·A·s are in the rising sector, as they show excellent magnetocaloric responses and, among all H·A·s, have better mechanical resistance than those containing *p*-block elements.[44–49] The last few on the list are the FeRh, $Gd_5Si_2Ge_2$, and RE_2In families. Though the FeRh and $Gd_5Si_2Ge_2$ families have undergone extensive research, the former remains in pursuit of understanding the largest adiabatic temperature change among magnetocaloric materials[50–55] while the latter for managing hysteresis or fabricating them as composites.[56–58] Their use of critical elements, such as Gd, Ge, and Rh, in the designed compositions greatly diminished their significance (symbols are in blue). Even though the RE_2In family also employs critical elements in large proportions, it is in the growing sector due to several reasons: their large MCE due to a FOMT have no detrimental hysteresis, which is first reported recently (in 2018);[59] excellent performance at low temperatures, which correspond to the current research area of interest for H_2 or N_2 liquefaction range.[60,61]

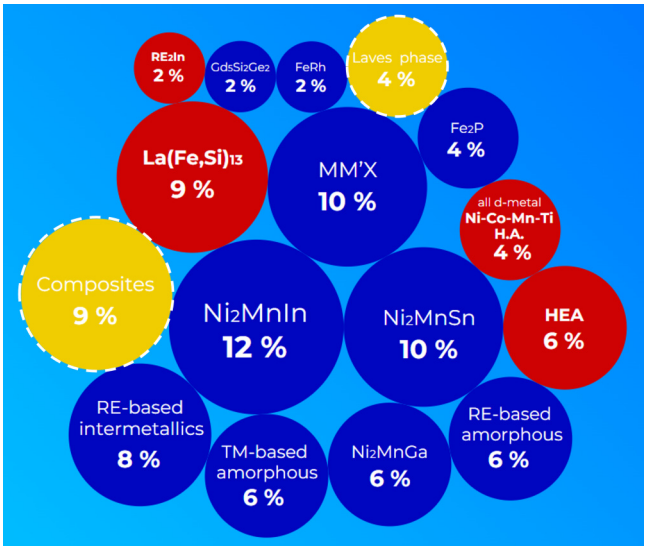

FIG. 1. Bubble chart of the popular choices of magnetocaloric material families published during 2019–2022. Sizes of the bubbles correspond to the percentage of the annual papers published. Each family of materials is further analyzed by the symbol color: red as increasing publications, yellowish represent constant while blue as declining sectors. WoS literature survey was performed under search terms, "magnetocaloric," "material," and "alloy."

III. THE OPEN QUESTIONS

Among these "trendy" materials, there are open questions that require investigation and resolution to achieve optimal performance and, therefore, push MR technology forward. As mentioned previously, GMCE ascribed to FOMT usually results in hysteresis, decreasing the materials' cyclic responses and their suitability as refrigerant working materials. However, one of the most challenging aspects of optimization is reducing hysteresis without compromising magnetocaloric performance. In addition, an accurate description of the phase transitions of the materials becomes crucial due to the associated hysteresis management. Also, it is

possible to optimize magnetocaloric performance by identifying the critical composition of FOMT crossovers to SOMT as it achieves the best characteristics of both classes: the largest MCE among its SOMT compositions with negligible hysteresis. Despite this, conventional methods for evaluating thermomagnetic phase transitions can be ambiguous in certain cases, hindering the identification of the critical composition.

A further open question for FOMT materials is that they often display mechanical instabilities due to the accompanying volume changes during the transition, which negatively impacts both long-term durability and machining. Additionally, most FOMT materials are inevitably obtained in the presence of undesirable secondary phases, which jeopardize the assessment of the performance of pure phases.

Proposed hypotheses for addressing these open questions will be made in Secs. IV and V, which will be divided into materials design and characterization analyses and methods.

IV. MATERIALS DESIGN

A. Hysteresis entailed to FOMT addressed by microstructural manipulation

The accompanying hysteresis due to FOMT aggravates the resultant cyclic values and device performance. Thus, attempts to retain large MCE with small/negligible hysteresis are an ongoing effort of the community despite the development of many upcoming GMCE materials.[28,37,49,62–64] One way to achieve negligible hysteresis is to switch to SOMT magnetocaloric materials. However, this leads to substantial compensation for the magnitude of MCE one could get (note that the benchmark MCE material for room temperature is still Gd[5]). Moreover, magnetic fields can reduce thermal hysteresis, so changing the order of the transition from FOMT to SOMT is not required for effective cyclic responses. These responses can be improved by fine-tuning the character of the transition, i.e., when approaching the critical composition. The closer SOMT materials are to the critical composition, regardless of the magnetic field change used, the better.

It has been recently highlighted that microstructural control could manage the hysteresis of FOMT-La(Fe,Si)$_{13}$ compounds.[28] The authors found that the pristine La(Fe,Si)$_{13}$ sample shows a similar microstructure before and upon hydrogenation [see the bright field transmission electron micrographs presented in Figs. 2(a) and 2(b)]. The dissimilarity in the microstructures is observed with Ce additions, prior to [Fig. 2(c)] and after hydrogenation and weak and diffused reflections are observed (as indicated by the arrow) in the selected area electron diffraction (SAED) of (La,Ce)(Fe,Si)$_{13}$. Nanograin precipitation [circled in dashed line in Fig. 2(d)] is observed in the main 1:13 phase after hydrogenating (La,Ce)(Fe,Si)$_{13}$. The magnetic isotherms reveal that the initial FOMT-hysteresis [Fig. 2(e)] significantly diminish while retaining FOMT-character upon hydrogenation [Fig. 2(f)]. The peak isothermal entropy change, $|\Delta S^{peak}_{isothermal}|$, of hydrogenated (La,Ce) (Fe,Si)$_{13}$ sample is 10.8 J kg^{-1} K^{-1} for 1 T (15.6 J kg^{-1} K^{-1} for 2 T), which is considered a large magnitude for low magnetic fields.

A different approach has been proposed to reduce hysteresis by adjusting the geometric compatibility of the crystal structures involved in the magnetostructural phase transition through composition modifications. This was reported for MM'X[62] and Heusler alloy families,[49,63] which undergo magnetostructural transitions with promising magnetocaloric responses. The decreased hysteresis was ascribed to the reduction of elastic and interfacial energy of the transition though it should be noted that the observed hysteresis is still significant.

B. Mechanical instabilities due to FOMT/intermetallic character

1. HEA design strategy

When it comes to developing materials with good mechanical properties, the HEA design concept is a popular choice today since its exceptional mechanical characteristics could exceed those of

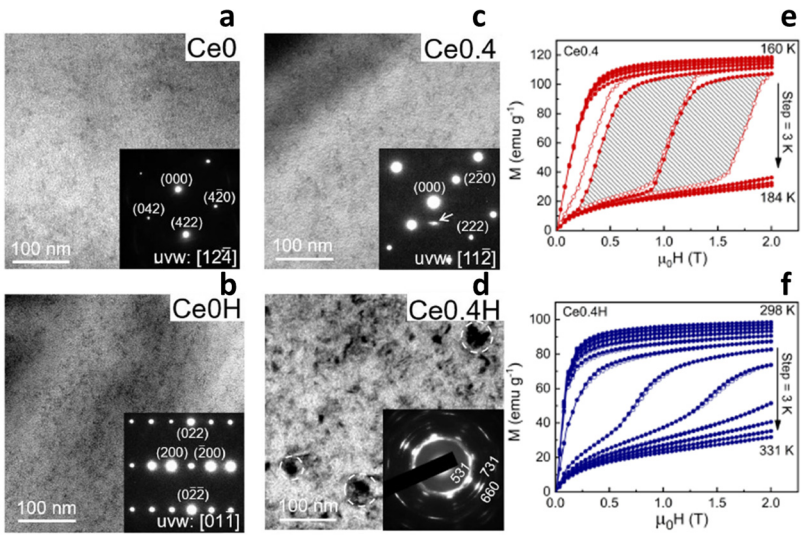

FIG. 2. Microstructure for pristine La(Fe,Si)$_{13}$ sample is similar prior to (a) and after (b) hydrogenation. Ce-doped La(Fe,Si)$_{13}$ sample shows weak and diffuse reflections in the SAED pattern (indicated by arrow) (c) and a dissimilar microstructure upon hydrogenation (d). Nanograin precipitation (circled in dashed lines) observed in the 1:13 matrix. The magnetization and demagnetization isotherms show that the large hysteresis observed in Ce-doped La(Fe,Si)$_{13}$ (e) has significantly decreased after hydrogenation (f). Reproduced with permission from Liu *et al.*, Acta Mater. **207**, 116687 (2021). Copyright 2021 Elsevier.

traditional alloys. As the concept involves multiprincipal alloying elements rather than adding trace amounts to one or two main components, the large HEA compositional range opens up a range of potential properties to explore. Considering these advantages, it is particularly appealing to use the HEA design concept to develop novel magnetocaloric materials since the millennia-old method of alloy development is nearing maturity. Essentially, there should be a region in the HEA space with a unique combination of optimized MCE + mechanical properties that can address the structural instabilities faced by conventional magnetocaloric materials.

The works on magnetocaloric HEAS, as with their structural endeavors, so far have mostly focused on equiatomic compositions as well as increasing the number of elements in the central region of the multiprincipal elements phase diagram. This approach is not practical for magnetocaloric applications because it can cause the overall magnetization of the alloy to dilute, as if "too many cooks spoil the soup". In the recent review paper on HEA design strategies for magnetocalorics,[17] Law and Franco put together the comparison of magnetocaloric equiatomic vs non-equiatomic HEA reports as shown in Fig. 3. For those containing RE elements [Fig. 3(a)], they are typically limited to low temperature range (<75 K) for equiatomic compositions (solid circles). On the contrary, most of the non-equiatomic RE-containing HEAs (open circles) are found with transition temperatures ($T_{transition}$) above 75 K. In Fig. 3(b), equiatomic RE-free HEAs (solid circles) show extremely small MCE values, typically <0.6 J kg^{-1} K^{-1} for 2 T (see the magnified inset). Their non-equiatomic reports (open circles) undergoing SOMT show an order of magnitude enhancement while those with FOMT have excellent MCE magnitudes up to 10.2 J kg^{-1} K^{-1} (2 T).[65]

This large MCE enhancement found for RE-free non-equiatomic HEAs corresponds to Fe–Mn–Ni–Ge-Si HEAs,[65,66] which undergo FOMT. Their composition designs were sought using a targeted-property method, which prompted recent review papers[17,18] to emphasize the importance of effective search strategies for exploring the vast HEA compositional space. The search approach originated from a parent composition, MnNiSi, for exhibiting a first-order phase transition from orthorhombic ↔ hexagonal structures. Based on the parent stoichiometry, the compositional design was geared toward the non-equiatomic HEA regions with the addition of compatible chemical elements in appropriate proportions. In this way, the vast non-equiatomic HEA space can be searched rationally and efficiently. The design approach in Ref. 67 was similar, but the introduction in Refs. 65 and 66 of an additional criterion of chemical compatibility allows to maximize configurational entropy of mixing: the non-equiatomic Fe–Mn–Ni–Ge–Si HEAs deliver a configurational entropy of mixing close (99%) to the maximum for a quinary alloy and maintain a 2:1 ratio of TM element to *p*-block element. The MCE of these Fe–Mn–Ni–Ge–Si HEAs[65,66] closes the pre-existing gap between magnetocaloric HEAs vs conventional high-performing magnetocaloric materials as shown in Fig. 4(a). Further analysis of normalizing to the largest $|\Delta S^{peak}_{isothermal}|$ value [26. 8 J kg^{-1} K^{-1} (2 T) from La(Fe,Si)$_{13}$ family] presented as an infographic in Fig. 4(b) shows that Fe–Mn–Ni–Ge–Si HEAs can exhibit potential for MCE. This breakthrough reassures that the combined functional and mechanical properties with the HEA design concept are not a pipe dream.

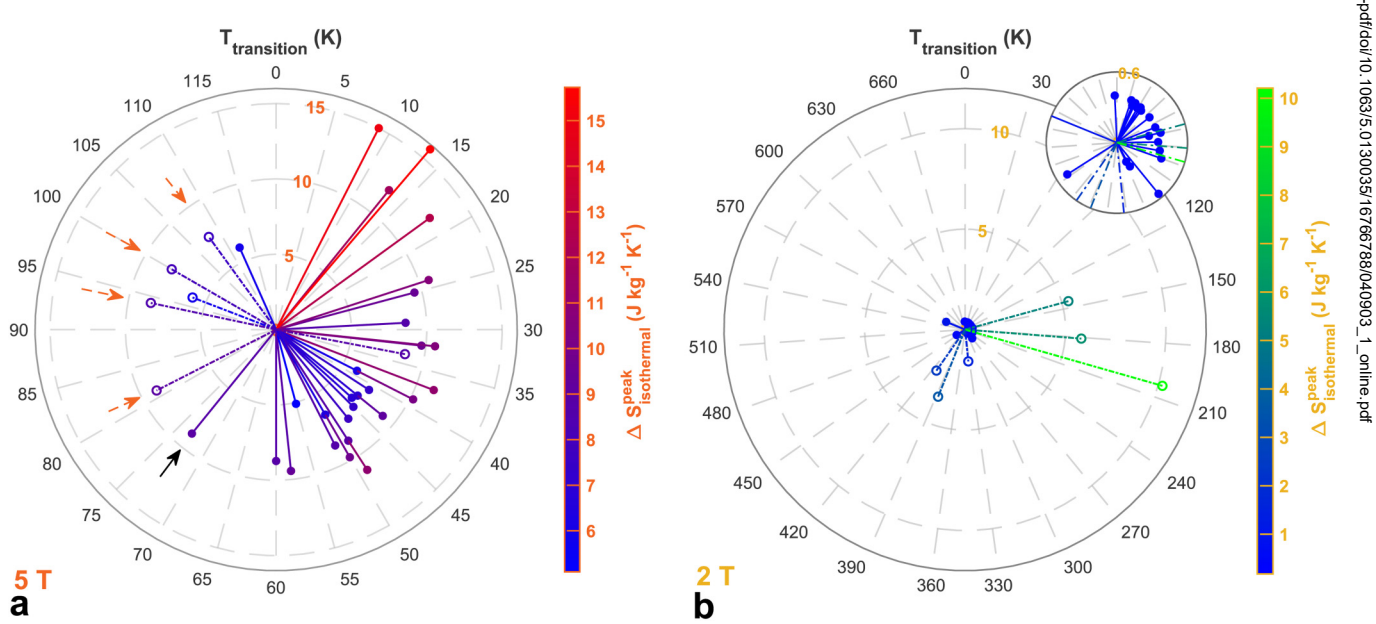

FIG. 3. Comparison of the MCE performance of HEAs: (a) RE-amorphous (5 T) and (b) RE-free HEA (2 T). Solid circles are those with equiatomic compositions while open circles are for the non-equiatomic HEAs. Black arrow in (a) panel marks the equiatomic GdTbCoAl vs its non-equiatomic counterparts (orange arrows). Inset in (b): A subplot with a smaller scale axis for the performance of equiatomic RE-free HEAs. Image reproduced with permission from J. Y. Law and V. Franco, J. Mater. Res. (published online) (2022). Copyright 2022 Author(s), licensed under an open access Creative Commons CC BY license.

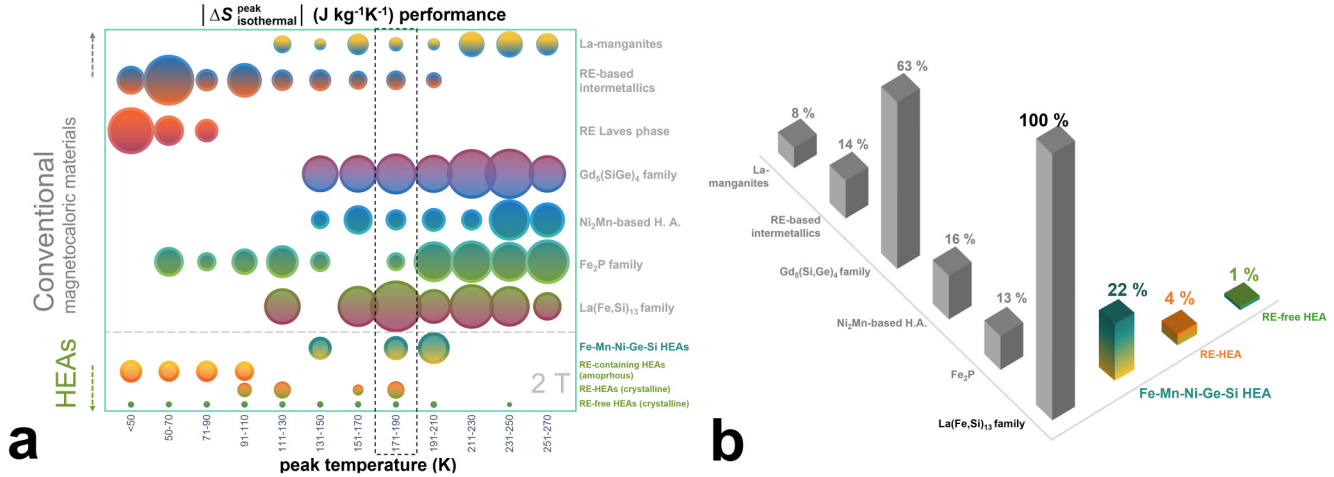

FIG. 4. (a) MCE performance matrix (using $|\Delta S^{peak}_{isothermal}|$ and its corresponding temperature) for 2 T: magnetocaloric HEAs (greenish text) vs conventional magnetocaloric materials (gray text), further differentiated by the dashed line. Size of the circles corresponds to the magnitude of $|\Delta S^{peak}_{isothermal}|$. (b) An infographic of the normalized MCE performance of the magnetocaloric materials marked in the boxed region of panel (a). Data are gathered from Refs. 5,12,17,18,33,37,42,65,66, and 68–87.

2. Composites strategy

Designing composite system for magnetocalorics has been a popular choice for performance optimization, especially for extending the temperature span of the regenerators. Ideally, this is done by arranging magnetocaloric materials in the order of their thermomagnetic phase transition temperatures, which has also been experimentally validated to optimize performance. Additional considerations, such as thermal contact and the proximity of these transition temperatures, should not be disregarded. This is also true for the phase proportions of multiphase magnetocaloric composites in a single bulk composition. The details of such efforts have recently been compiled in Ref. 16, which emphasizes the importance of making necessary efforts in order to properly achieve performance optimization. Moreover, this review discusses composites as multifunctional composites, where the magnetocaloric material is combined with a polymer or metal binder to provide structural stability to regenerators. The majority of these efforts are directed at the family of $La(Fe,Si)_{13}$ alloys.[88–91] A further study on their characterization in test devices (including modeling investigations) was reported for epoxy-bonded $La(Fe,Mn,Si)_{13}H_y$ particles and their multi-layered regenerators.[92,93] During a 2-month discontinuous test, the composite regenerators were reported to show good stability without failure.[92] Later, the authors were able to achieve successful 1-year tests of non-bonded composites of $La(Fe,Mn,Si)_{13}H_y + \alpha$-Fe content.[94] Besides the interest of structural stability in their magnetocaloric composite regenerators, they also highlighted the importance of well-adjusted temperature distribution along the composite-layered active magnetic regenerators to ensure that all the layers are fully utilized to achieve performance optimization.

Very similarly, a recent report used a secondary phase at the grain boundaries of Ni–Mn–In–(Fe) Heusler alloys that hindered intergranular fracture during cyclic loading, leading to a >3 orders of magnitude increase in cyclic stability over the single-phase alloy.[95] This is in contrast with trace doping, which has been reported to manage the deformation in Heusler alloys and is not included here because it is less exotic than the favored additional phase incorporation for secondary properties. Similar findings were also reported for $Ni_{45}Co_5Mn_{37}(In,Gd)_{13}$ and $Mn_{49}Ni_{41}(Sn,Gd)_{10}$ alloys, where the Gd-rich secondary phase was found to enhance mechanical properties.[96,97] When simultaneously grain boundary strengthening by NiBH clusters is combined with grain refinement, the mechanical properties of Ni–Mn-based multifunctional alloys are greatly enhanced.[98]

Due to current concerns about a decarbonized hydrogen society, magnetocalorics is currently being pursued for H_2 liquefaction. The hydrogen gas is precooled to ~77 K (liquid nitrogen temperature) before being chilled down to 20 K in this process. Hence, H_2 liquefaction cannot be accomplished in a single magnetocaloric material, even if it is highly efficient (MCE is at maximum near the thermomagnetic phase transition, thus is restricted to a limited temperature span). $RECo_2$ (RE = Ho and Er) Laves phases have shown to exhibit tunable large MCE over a range of 20–77 K,[38] which may help address the bottleneck temperature range. Additionally, the authors further optimized the performance by reducing hysteresis for Fe and Ni substitutions. Combination of these phases would be a possible way of developing composites for this temperature range.

3. Additive manufacturing

The poor processability of high-performance magnetocaloric regenerators can be addressed by using emerging additive manufacturing (AM) techniques. In contrast to traditional manufacturing methods, AM allows the fabrication of products with final geometries, minimizing material waste, time, and tool cost, as well as eliminating the net-shaping stages. As a result, magnetocaloric

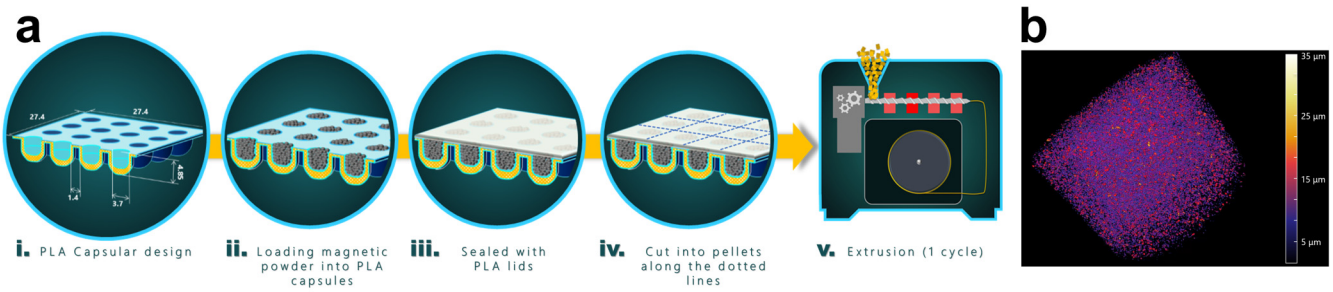

FIG. 5. (a) Methodology for developing own magnetocaloric filaments with desired magnetocaloric filler compositions. (b) X-ray tomography results show a uniform filler distribution, validating the proof-of-concept methodology.

regenerators with complex geometric designs can be made for magnetic refrigerators.

Among the different AM techniques, fused deposition modeling (FDM) stands out because it does not melt the magnetocaloric material during the process (manufacturing temperatures are below the melting points of alloys), allowing the final product to retain the FOMT functionality needed for large MCE. Nevertheless, it must feed filaments of excellent quality and uniformity to carry out high-resolution 3D printing. Such a challenge has been addressed by a unique feedstock that consists of customized polylactic acid (PLA) encapsulated metallic fillers that produce high-quality magnetic composite filaments with a uniform dispersion for printing high-resolution objects.[99,100] Figure 5(a) shows a schematic of this innovative feedstock design, its preparation, and filament extrusion. The homogeneity of the magnetic filler dispersion in the PLA matrix is observed using x-ray tomography of the resultant composite filament, as shown in Fig. 5(b). Upon optimizing the compositions of the composite filaments, this methodology was utilized to fabricate magnetocaloric composite filaments of PLA + La(Fe, $Si)_{13}$-family for 3D printing.[101] An *in situ* assessment of the magnetocaloric response of the printed object revealed that the magnetocaloric response of the fillers is not affected by the manufacturing procedure.

A recent study found that additively manufactured $Co_{49}Ni_{21}Ga_{30}$ ferromagnetic shape memory alloys using laser power bed fusion (L-PBF) and direct energy deposition (DED) exhibit martensitic transformation similar to as-cast counterpart.[102] Except for the modification of the saturation magnetization and magnetization response with respect to temperature (i.e., dM/dT) observed in L-PBF samples, the thermomagnetic behavior of the DED sample is similar to that of as-cast counterpart, which indicates it as a successful case (see Fig. 6).

V. NEWLY IMPLEMENTED ANALYSIS METHODS/ MODELS

A. Exponent *n* criteria

One very common analysis performed on evaluating magnetocaloric materials is determining the order of their thermomagnetic phase transitions: whether they are FOMT or SOMT. The methods of determining them have revolved around the magnetocaloric curve shapes, the presence of thermal hysteresis, universal curve scaling,[103] and Banerjee's criterion.[104] Except for the latter, all are based on subjective interpretations by different evaluators, where the observation of thermal hysteresis can be a particularly tricky case due to the thermal lag experienced by the sample during the measurements. Banerjee's criterion is helpful in clarifying interpretations, but it has been found inapplicable in several instances, resulting in erroneous interpretations of other complementary techniques (see Ref. 105).

The above-mentioned limitations have been addressed by the discovery of a FOMT fingerprint reported in Ref. 106. Law *et al.* demonstrated that the field dependence exponent n criterion clearly distinguishes for FOMT when there is an overshoot of $n > 2$ near the transition temperature while its absence indicates either a SOMT or the critical point where FOMT crossovers to SOMT. A

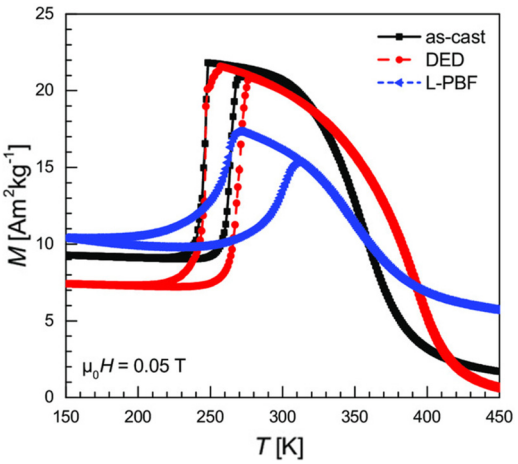

FIG. 6. Thermomagnetic behavior of $Co_{49}Ni_{21}Ga_{30}$ ferromagnetic shape memory alloys in as-cast, DED, and L-PBF states at 0.05 T. Image is reproduced from Scheibel *et al.*, Adv. Eng. Mater. 24, 2200069 (2022). Copyright 2022 Author(s), licensed under an open access Creative Commons CC BY license.

summary of the criterion identifying these different regimes is presented in Fig. 7 using simulations from the Bean and Rodbell model[107] with varying η parameters (η < 1 for SOMT; η = 1 for critical point; η > 1 for FOMT). For all cases, exponent n shows a value of 1 at low temperatures due to the initial ferromagnetic (FM) state of the sample. It proceeds toward a minimum when arriving at the transition temperatures except for η > 1, where overshoots of $n > 2$ (color shaded) are observed immediately after the minima. The latter is the fingerprint of FOMT. Finally, exponent n saturates to the value of 2 with increasing temperatures in all cases, ascribed to reaching the paramagnetic (PM) state of the sample. In Ref. 106, the authors applied their discovery to theoretical calculations as well as several experimental case studies:

- Magnetoelastic phase transitions [using a series of $La(Fe,Si)_{13}$ with varying compositions for FOMT → SOMT],
- Distribution of transition temperatures in FOMT systems [several FOMT-$La(Fe,Si)_{13}$ composites with distributed transition temperatures],
- Magnetostructural phase transformation (martensitic → austenitic transitions of FOMT-type in Heusler alloys),
- Antiferromagnetic → ferromagnetic phase transitions (using $GdBaCo_2O_{6-\delta}$ cobaltite perovskites).

Furthermore, the authors also reported that the minimum of exponent n at the transition temperatures ($n_{transition}$) can be used as another criterion to determine the critical point where FOMT → SOMT.[108] The main panel in Fig. 7 illustrates this criterion, where $n_{transition} = 0.4$ at the critical point (η = 1).

In addition, the coauthors further found that samples undergoing anti-FM to PM transitions show exponent n beginning at values of 2 at low temperatures, where the sample is in the anti-FM state.[109] It must be noted that the FOMT fingerprint is not applicable in the temperature range where inverse MCE (positive $|\Delta S_{isothermal}|$) switches to direct MCE (negative $|\Delta S_{isothermal}|$), in which the observed characteristics are reflected as the switching sign attributes (see "Highlights of some misconception and misuse of the criteria" below).

In general, the above has been applied to a wide variety of magnetocaloric materials, validating its capabilities in a wide range of scenarios, including complex ones such as tight overlaps in phase transitions of multiphase materials, and so on.[74,110] N. H. van Dijk[111] expanded the above-mentioned studies with the Landau model and found results to be in agreement with exponent n criteria, which further reinforced the breakthrough of exponent n criteria[106,108] made to the determination of the order of phase transitions within the magnetocaloric community.

Highlights of some misconception and misuse of the criteria: As n is calculated from

$$n\,(T, H) = \frac{d \ln |\Delta S_{\text{isothermal}}|}{d \ln H},$$

where T = temperature and H = magnetic field, appropriate determination of $|\Delta S_{isothermal}(T, H)|$ data is well appreciated to avoid obtaining artifacts or noisy n results, compromising the MCE evaluation thereafter. A very common issue is to dismiss the effects of

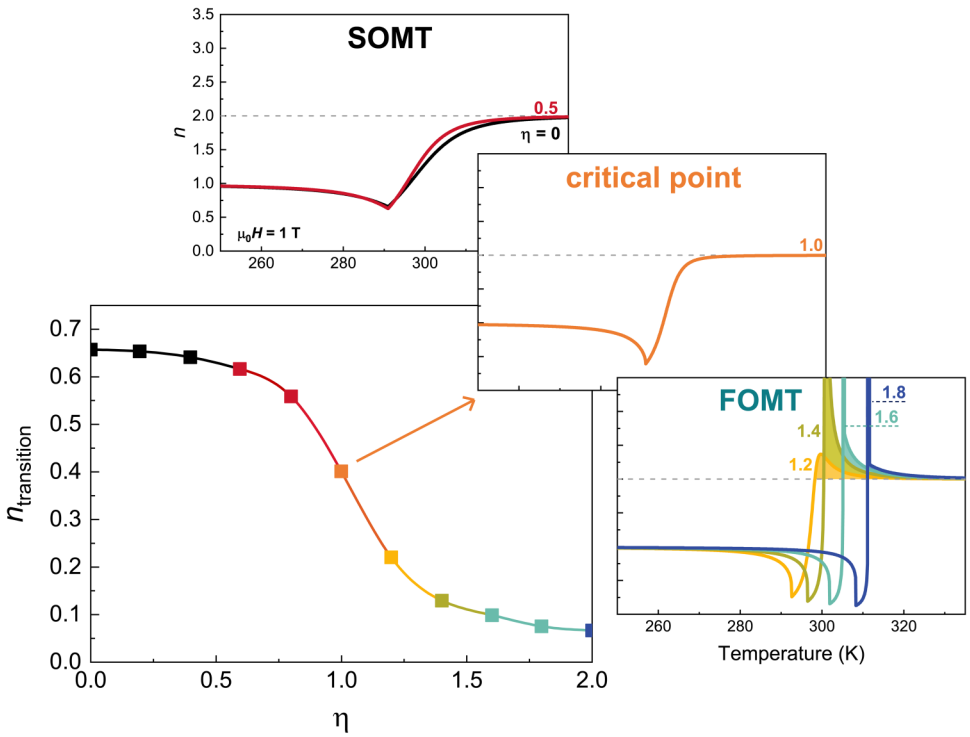

FIG. 7. Exponent n criterion for determining SOMT (η < 1), critical point (η = 1), and FOMT (η > 1). Overshoot as FOMT fingerprint is further color shaded.

the demagnetizing factor on $|\Delta S_{isothermal}(T, H)|$ data, which can significantly affect the results for low magnetic fields. The low-magnetic field behavior gives crucial information on the presence of impurities affecting the MCE and interpretation of the order of the phase transition.

Furthermore, it is recommended to verify the $n(T, H)$ results with the original $|\Delta S_{isothermal}(T, H)|$ data on the same temperature scale axis, as presented in Fig. 8 (the appropriate FOMT overshoot is shaded in yellowish color). This is because when the $\Delta S_{isothermal}(T, H)$ switches from negative to positive sign or vice versa, it can give the characteristic features of sign-switching, which can be misinterpreted as the characteristic FOMT overshoot, as highlighted in the pattern-filled region in Figs. 8(c) and 8(d). In other words, the initial proper determination of $|\Delta S_{isothermal}(T, H)|$ data prior to n calculations is crucial to avoid as many artifacts as possible.

B. Hysteresis studies/analysis using the TFORC technique

First Order Reversal Curve (FORC) distributions have been employed to further characterize magnetic hysteresis of magnetic materials.[20] This analysis technique was developed in 1999 by Pike, who proposed to magnetically characterize natural samples.[112] Each magnetic mineral has an associated FORC diagram and, therefore, can be used for identifying magnetic minerals in natural rocks. Since then, the FORC technique has been widely used in the community for revealing magnetization processes (either reversible or irreversible) and magnetic interactions, which are not clearly identified from major hysteresis loops.[113–115]

This analysis technique has recently been extrapolated to characterize the thermal hysteresis of first-order magnetocaloric materials, termed Temperature First Order Reversal Curve (TFORC) technique.[116,117] It enables the identification of inhomogeneities,[116] asymmetry in transformations (such as asymmetric transformation rates of the cooling/heating branch or different characteristics in the cooling and heating procedures), and different phenomena, such as kinetic arrest.[118] These are very relevant for the performance evaluation of magnetocaloric materials, as any change to those features could lead to improved magnetocaloric performance. By employing a phenomenological approach, a catalog of various characteristic TFORC distributions of first-order magnetocaloric materials can be obtained[119] as shown in Fig. 9. Even though the difference in the major loops is not as obvious, it gets magnified in the TFORC distributions. The distribution adopts a circular shape as shown in Fig. 9(a) when it corresponds to a completely

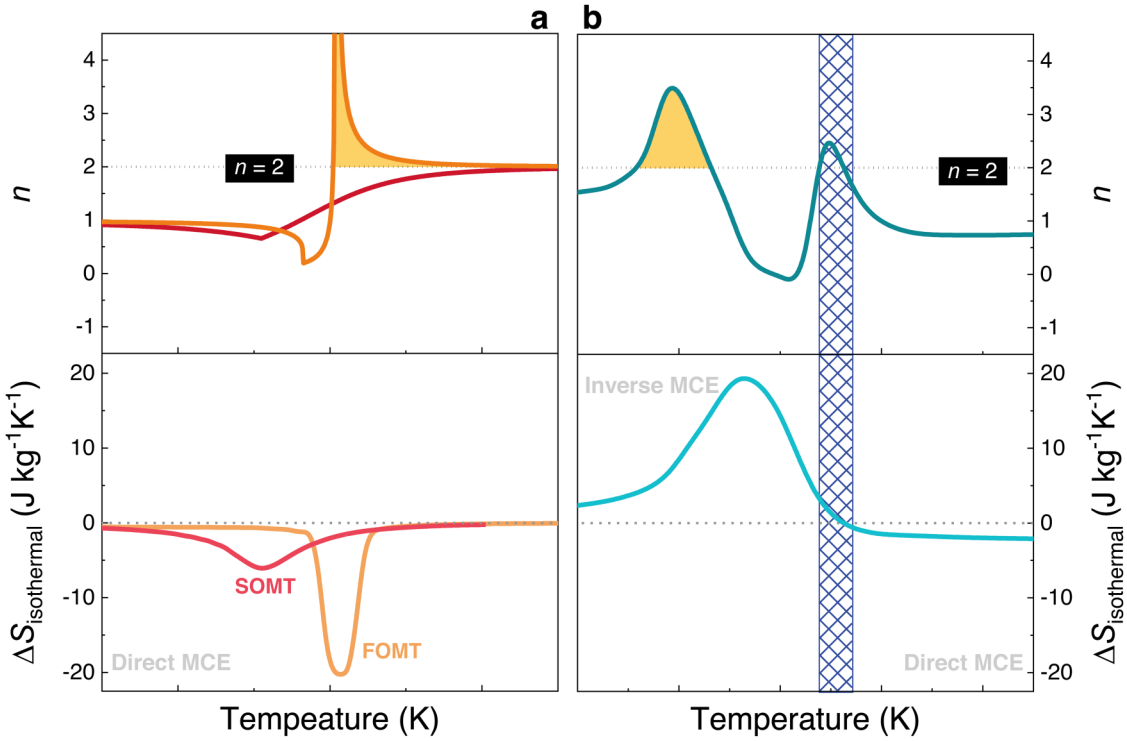

FIG. 8. Schematic illustration of the temperature dependence of (top panel) exponent n calculated from their corresponding (bottom panel) $\Delta S_{isothermal}$ data. The overshoot of $n > 2$ fingerprinting the FOPT in (a) direct and (b) inverse MCE is further highlighted in yellowish color. The pattern-filled region in (b) demonstrates a characteristic $n(T)$ feature resulting from the sign-switching of $\Delta S_{isothermal}$ and should not be construed that it meets the FOMT criterion. Image adapted with permission from J.Y. Law and V. Franco, J. Mater. Res. (published online) (2022). Copyright 2022 Author(s), licensed under an open access Creative Commons CC BY license.

symmetric transformation. As the asymmetry in the transformations increases, the circular distribution distorts to ellipse [Fig. 9(b)]→ semi-circle/semi-ellipse [Fig. 9(c)] → triangle-like shape [Fig. 9(d)]. For all the distributions, the distortion will depend on the degree of asymmetry and the possible combinations of the heating/cooling transformations. Furthermore, it is possible to correlate the TFORC distributions with reversible (or cyclic) magnetocaloric performance,[120] which helps optimize materials.

C. Phase deconvolution

Recently, the universal scaling of the magnetocaloric effect, first reported by Franco,[121] has been further investigated and extended to deconvolute the magnetocaloric behavior of multiphase magnetocaloric composite systems. For systems of two SOMTs [depicted as phases A and B in Fig. 10(a)] whose Curie transitions overlap each other (solid lines), deconvolution can enable the prediction of the magnetocaloric responses of each phase (as presented in shaded regions) from which the total response of the multiphase sample can be recovered (dashed lines). In short, the proposed deconvolution procedure as reported in Ref. 122 adopts the application of the scaling laws to the total response of the multiphase sample, considering separately each of the $\Delta S_{isothermal}$ peaks. In situations of tight overlap as the case shown in Fig. 10(a), each SOMT can significantly affect the temperature range where the other SOMT takes place. These cross-effects can be effectively corrected by comparing the reconstructed responses and the experimental curves.

The same authors also applied this deconvolution procedure to systems with FOMT + SOMT,[123] which is a common scenario of Heusler alloys, whose martensitic and austenitic phases can result in inverse and direct MCE as shown in Fig. 10(b). Figure 10(c) shows that upon the deconvoluted SOMT arising from the Curie transition of the austenitic phase, proper MCE evaluation of the inverse MCE arising from the FOMT is enabled [as compared to the region highlighted in blue in Fig. 10(b)]. For further details on the other applications of the scaling laws, readers are recommended to refer to Refs. 19, 20, and 103.

D. Machine learning models

As high-throughput methods have gained increasing traction in recent years, machine learning (ML) has become a very popular choice, as it is able to analyze large amounts of data to explore relationships among physical properties or find materials with desirable properties.[124,125] ML tools are designed to use statistical analyses from massive amounts of experimental data without specific programming to create predictive models between selected properties. Magnetocaloric materials have only recently seen these efforts, with promising results. Aided by ML analyses, HoB_2 was discovered with GMCE at cryogenic temperatures.[126] Other studies also try to correlate and predict magnetocaloric materials by employing databases from first principle calculations.[127] For well-known magnetocaloric materials, such as Fe_2P, $La(Fe,Si)_{13}$,and manganite families, ML enables the extension of low-temperature limits[72] or correlates magnetocaloric responses, transition temperatures, or hysteresis while tuning compositions for room-temperature applications.[128–130] Although it may seem that designing materials using ML is a common practice today, it must be noted that the reliability of its predictions depends on both the number of phases in the database and on the reliability of the materials included (whether experimental or simulated from first principles). Therefore, the acquisition of data remains crucial for calculations.

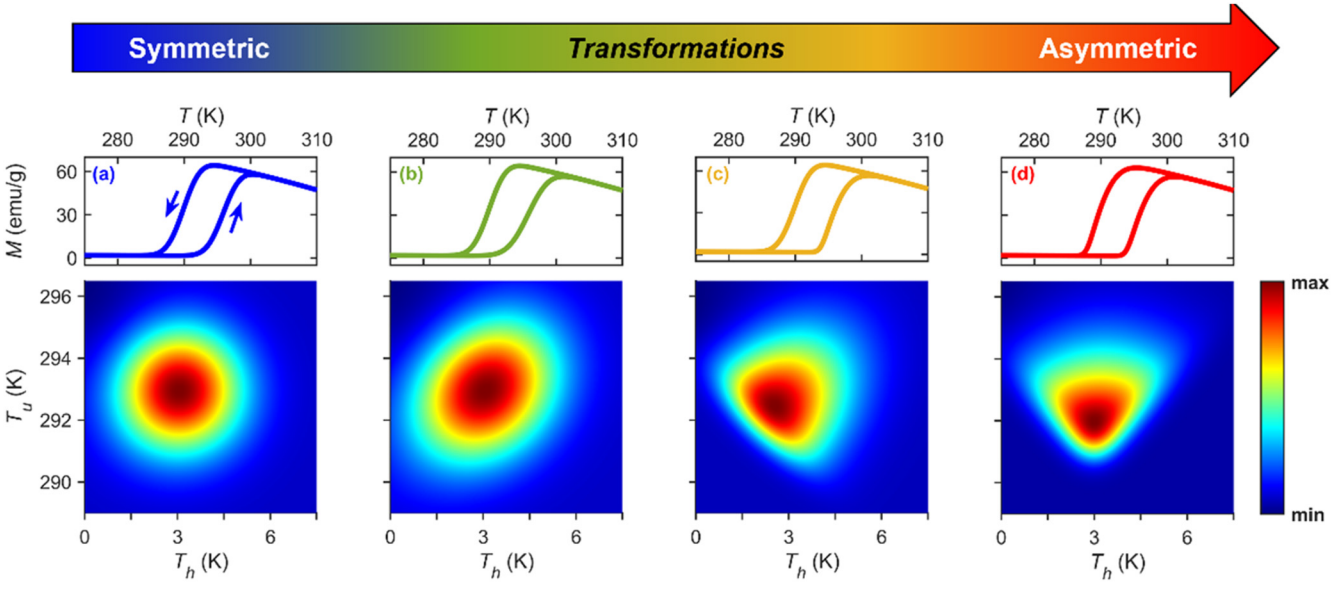

FIG. 9. Example of different TFORC distributions plotted vs the T_h and T_u variables that indicate the width and the center of the loops, respectively, according to the change in transition. Further details can be found in Ref. 119.

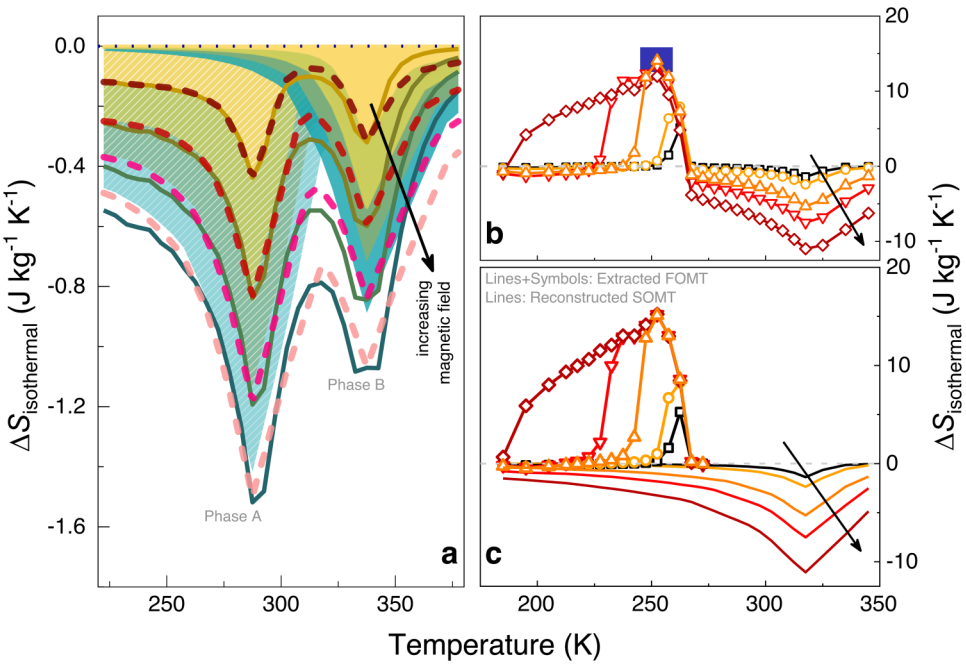

FIG. 10. The application of the deconvolution method to (a) SOMTs where the shaded regions are their deconvoluted phases. For FOMT + SOMT system with the (b) MCE of their martensitic and austenitic phases and (c) their extracted MCE behavior upon deconvolution. Arrow depicts increasing magnetic fields.

VI. FUTURE OUTLOOK

Materials in trend have evolved over the years since the advent of magnetocaloric research in the nineties of the previous century. Gd, as a second-order phase transition material, remains the *de facto* benchmark for applications, while others with a first-order phase transition exhibit better performance in the laboratory but lack some of the secondary properties needed to be effectively implemented in a device. Among the most relevant challenges are the improvement of mechanical stability, reversibility (associated with a decrease in thermal hysteresis), phase purity, and formability. These must be tackled by a combination of advanced characterization methods and the development of new materials with the help of computer-guided techniques, such as machine learning/artificial intelligence. Among the materials gaining new interest due to their expected favorable mechanical properties, which facilitate applicability, we highlight FOMT high entropy alloys and all-*d*-metal Heusler alloys, which also show promising magnetocaloric responses. However, to achieve peak performance, the hysteresis that these materials currently exhibit must be significantly reduced. Formability and processing are addressed by the development of composites and additive manufacturing. With respect to analysis techniques, the prediction of compositions at the separation between FOMT and SOMT can be quantitatively done nowadays and that could be instrumental in identifying compositions with enhanced performance. To facilitate the advancement toward the implementation of MR devices suitable for industrial and household appliances, a deeper characterization of the complementary properties of the materials, such as cyclability and stability, will also be needed.

ACKNOWLEDGMENTS

This work was supported by Grant PID2019-105720RB-I00 funded by MCIN/AEI/10.13039/501100011033, Consejería de Economía, Conocimiento, Empresas y Universidad de la Junta de Andalucía (Grant No. P18-RT-746), and U.S. Air Force Office of Scientific Research (No. FA8655-21-1-7044). J.Y.L. acknowledges an EMERGIA Fellowship from Junta de Andalucía.

AUTHOR DECLARATIONS

Conflict of Interest

The authors have no conflicts to disclose.

Author Contributions

Jia Yan Law: Conceptualization (equal); Data curation (equal); Formal analysis (equal); Investigation (equal); Visualization (equal); Writing – original draft (equal). **Luis M. Moreno-Ramírez:** Data curation (equal); Formal analysis (equal); Investigation (equal); Writing – review & editing (equal). **Álvaro Díaz-García:** Data curation (equal); Formal analysis (equal); Investigation (equal); Writing – review & editing (equal). **Victorino Franco:** Conceptualization (equal); Data curation (equal); Formal analysis (equal); Funding acquisition (equal); Investigation (equal); Writing – review & editing (equal).

DATA AVAILABILITY

The data that support the findings of this study are available from the corresponding author upon reasonable request.

REFERENCES

[1]U. S. Environmental Protection Agency, *Climate Change Indicators: Residential Energy Use* (EPA, 2021), https://www.epa.gov/climate-indicators/climate-change-indicators-residential-energy-use (updated by April 2021).

[2]IEA, *The Future of Cooling* (IEA, Paris, 2018), https://www.iea.org/reports/the-future-of-cooling.
[3]Enerdata, *Global Energy Trends - 2021 Edition* (2021), https://www.enerdata.net/publications/reports-presentations/2021-energy-climate-trends.html
[4]C. B. Smith and K. E. Parmenter, in *Energy Management Principles*, 2nd ed., edited by C. B. Smith, and K. E. Parmenter (Elsevier, Oxford, 2016), p. 125.
[5]V. Franco, J. S. Blazquez, J. J. Ipus, J. Y. Law, L. M. Moreno-Ramirez, and A. Conde, Prog. Mater. Sci. **93**, 112 (2018).
[6]A. Kitanovski, Adv. Energy Mater. **10**, 1903741 (2020).
[7]O. Gutfleisch and V. Franco, Scr. Mater. **67**, 521 (2012).
[8]X. Moya and N. D. Mathur, "A hot future for cool materials," Front. Energy (published online) (2022).
[9]P. Weiss and A. Piccard, J. Phys. Théor. Appl. **7**, 103 (1917).
[10]G. Jaeger, Arch. Hist. Exact Sci. **53**, 51 (1998).
[11]A. M. Tishin and Y. I. Spichkin, *The Magnetocaloric Effect and Its Applications* (Institute of Physics Publishing, Bristol, 2003).
[12]V. K. Pecharsky and K. A. Gschneidner, Phys. Rev. Lett. **78**, 4494 (1997).
[13]O. Gutfleisch, T. Gottschall, M. Fries, D. Benke, I. Radulov, K. P. Skokov, H. Wende, M. Gruner, M. Acet, P. Entel, and M. Farle, Philos. Trans. R. Soc., A **374**, 20150308 (2016).
[14]S. Dall'Olio, M. Masche, J. Liang, A. R. Insinga, D. Eriksen, R. Bjørk, K. K. Nielsen, A. Barcza, H. A. Vieyra, N. V. Beek, H. N. Bez, K. Engelbrecht, and C. R. H. Bahl, Int. J. Refrig. **132**, 243 (2021).
[15]T. Gottschall, K. P. Skokov, M. Fries, A. Taubel, I. Radulov, F. Scheibel, D. Benke, S. Riegg, and O. Gutfleisch, Adv. Energy Mater. **9**, 1901322 (2019).
[16]J. Y. Law and V. Franco, in *Encyclopedia of Materials Composites*, edited by D. Brabazon (Elsevier, Oxford, 2021), Vol. 2, p. 461.
[17]J. Y. Law and V. Franco, "Review on magnetocaloric high-entropy alloys: Design and analysis methods," J. Mater. Res. (published online) (2022).
[18]J. Y. Law and V. Franco, APL Mater. **9**, 080702 (2021).
[19]V. Franco, Á Díaz-García, L. M. Moreno-Ramirez, and J. Y. Law, in *Magnetic Cooling: From Fundamentals to High Efficiency Refrigeration*, edited by K. G. Sandeman and O. Gutfleisch (Wiley, 2023).
[20]V. Franco, in *Magnetic Measurement Techniques for Materials Characterization*, edited by V. Franco and B. Dodrill (Springer International Publishing, Cham, 2021), p. 697.
[21]V. Franco *Determination of the Magnetic Entropy Change from Magnetic Measurements: the Importance of the Measurement Protocol* (LakeShore Cryotronics, 2014), https://www.lakeshore.com/docs/default-source/software/vsm/mce-software/determination-of-the-magnetic-entropy-change-from-magnetic-measurements.pdf?sfvrsn=d14f68c1_2
[22]A. Kitanovski, J. Tušek, U. Tomc, U. Plaznik, M. Ožbolt, and A. Poredoš, *Magnetocaloric Energy Conversion: From Theory to Applications* (Springer, Cham, 2015).
[23]A. Planes, L. Manosa, X. Moya, T. Krenke, M. Acet, and E. F. Wassermann, J. Magn. Magn. Mater. **310**, 2767 (2007).
[24]E. K. Liu, W. Zhu, L. Feng, J. L. Chen, W. H. Wang, G. H. Wu, H. Y. Liu, F. B. Meng, H. Z. Luo, and Y. X. Li, EPL **91**, 17003 (2010).
[25]S. Fujieda, A. Fujita, and K. Fukamichi, Appl. Phys. Lett. **81**, 1276 (2002).
[26]A. Aznar, P. Lloveras, J.-Y. Kim, E. Stern-Taulats, M. Barrio, J. L. Tamarit, C. F. Sánchez-Valdés, J. L. Sánchez Llamazares, N. D. Mathur, and X. Moya, Adv. Mater. **31**, 1903577 (2019).
[27]J. Lai, H. Sepehri-Amin, X. Tang, J. Li, Y. Matsushita, T. Ohkubo, A. T. Saito, and K. Hono, Acta Mater. **220**, 117286 (2021).
[28]Y. Liu, X. Fu, Q. Yu, M. Zhang, and J. Liu, Acta Mater. **207**, 116687 (2021).
[29]T. Hashimoto, T. Kuzuhara, K. Matsumoto, M. Sahashi, K. Imonata, A. Tomokiyo, and H. Yayama, IEEE Trans. Magn. **23**, 2847 (1987).
[30]T. Hashimoto, T. Kuzuhara, M. Sahashi, K. Inomata, A. Tomokiyo, and H. Yayama, J. Appl. Phys. **62**, 3873 (1987).
[31]D. Guo, L. M. Moreno-Ramírez, C. Romero-Muñiz, Y. Zhang, J. Y. Law, V. Franco, J. Wang, and Z. Ren, Sci. China Mater. **64**, 2846 (2021).
[32]D. Guo, L. M. Moreno-Ramírez, J. Y. Law, Y. Zhang, and V. Franco, Sci. China Mater. **66**, 249 (2023).
[33]Y. Zhang, J. Alloys Compd. **787**, 1173 (2019).
[34]L. Li and M. Yan, J. Alloys Compd. **823**, 153810 (2020).
[35]TMS, *Defining Pathways for Realizing the Revolutionary Potential of High Entropy Alloys* (TMS, Pittsburgh, PA, 2021).
[36]L. Han, F. Maccari, I. R. Souza Filho, N. J. Peter, Y. Wei, B. Gault, O. Gutfleisch, Z. Li, and D. Raabe, Nature **608**, 310 (2022).
[37]J. Lai, X. You, J. Law, V. Franco, B. Huang, D. Bessas, M. Maschek, D. Zeng, N. van Dijk, and E. Brück, J. Alloys Compd. **930**, 167336 (2023).
[38]X. Tang, H. Sepehri-Amin, N. Terada, A. Martin-Cid, I. Kurniawan, S. Kobayashi, Y. Kotani, H. Takeya, J. Lai, Y. Matsushita, T. Ohkubo, Y. Miura, T. Nakamura, and K. Hono, Nat. Commun. **13**, 1817 (2022).
[39]Z. Zheng, H. Wang, C. Li, X. Chen, D. Zeng, and S. Yuan, Adv. Eng. Mater. **n/a**, 2200160 (2022).
[40]L. Luo, J. Y. Law, H. Shen, L. M. Moreno-Ramírez, V. Franco, S. Guo, N. T. M. Duc, J. Sun, and M.-H. Phan, Metals **12**, 1536 (2022).
[41]X. Miao, Y. Gong, F. Zhang, Y. You, L. Caron, F. Qian, W. Guo, Y. Zhang, Y. Gong, F. Xu, N. van Dijk, and E. Brück, J. Mater. Sci. Technol. **103**, 165 (2022).
[42]W. Liu, E. Bykov, S. Taskaev, M. Bogush, V. Khovaylo, N. Fortunato, A. Aubert, H. Zhang, T. Gottschall, J. Wosnitza, F. Scheibel, K. Skokov, and O. Gutfleisch, Appl. Mater. Today **29**, 101624 (2022).
[43]J. Lai, X. Tang, H. Sepehri-Amin, and K. Hono, Scr. Mater. **188**, 302 (2020).
[44]S. Liu, H. Xuan, T. Cao, L. Wang, Z. Xie, X. Liang, H. Li, L. Feng, F. Chen, and P. Han, Phys. Status Solidi A **216**, 1900563 (2019).
[45]A. Taubel, B. Beckmann, L. Pfeuffer, N. Fortunato, F. Scheibel, S. Ener, T. Gottschall, K. P. Skokov, H. Zhang, and O. Gutfleisch, Acta Mater. **201**, 425 (2020).
[46]Y. Li, S. Huang, W. Wang, E. Liu, and L. Li, J. Appl. Phys. **127**, 125501 (2020).
[47]A. N. Khan, L. M. Moreno-Ramírez, Á Díaz-García, J. Y. Law, and V. Franco, J. Alloys Compd. **931**, 167559 (2023).
[48]Y. Li, L. Qin, S. Huang, and L. Li, Sci. China Mater. **65**, 486 (2022).
[49]F. Zhang, I. Batashev, N. van Dijk, and E. Bruck, Phys. Rev. Appl. **17**, 054032 (2022).
[50]M. P. Annaorazov, S. A. Nikitin, A. L. Tyurin, K. A. Asatryan, and A. K. Dovletov, J. Appl. Phys. **79**, 1689 (1996).
[51]A. Chirkova, K. P. Skokov, L. Schultz, N. V. Baranov, O. Gutfleisch, and T. G. Woodcock, Acta Mater. **106**, 15 (2016).
[52]V. I. Zverev, A. M. Saletsky, R. R. Gimaev, A. M. Tishin, T. Miyanaga, and J. B. Staunton, Appl. Phys. Lett. **108**, 192405 (2016).
[53]Y. Zhang, J. Chen, K. Ikeda, K. Yamagami, Y. Wang, Y. Choi, A. Yasui, J. Ma, Y. Lin, C. Nan, and H. Wadati, J. Alloys Compd. **921**, 166080 (2022).
[54]R. R. Gimaev, A. A. Vaulin, A. F. Gubkin, and V. I. Zverev, Phys. Met. Metallogr. **121**, 823 (2020).
[55]K. Qiao, J. Wang, S. Zuo, H. Zhou, J. Hao, Y. Liu, F. Hu, H. Zhang, A. G. Gamzatov, A. Aliev, C. Zhang, J. Li, Z. Yu, Y. Gao, F. Shen, R. Ye, Y. Long, X. Bai, J. Wang, J. Sun, R. Huang, T. Zhao, and B. Shen, ACS Appl. Mater. Interfaces **14**, 18293 (2022).
[56]A. Biswas, Y. Mudryk, A. K. Pathak, L. Zhou, and V. K. Pecharsky, J. Appl. Phys. **126**, 243902 (2019).
[57]V. M. Andrade, A. Amirov, D. Yusupov, B. Pimentel, N. Barroca, A. L. Pires, J. H. Belo, A. M. Pereira, M. A. Valente, J. P. Araújo, and M. S. Reis, Sci. Rep. **9**, 18308 (2019).
[58]V. M. Andrade, N. B. Barroca, A. L. Pires, J. H. Belo, A. M. Pereira, K. R. Pirota, and J. P. Araújo, Mater. Des. **186**, 108354 (2020).
[59]F. Guillou, A. K. Pathak, D. Paudyal, Y. Mudryk, F. Wilhelm, A. Rogalev, and V. K. Pecharsky, Nat. Commun. **9**, 2925 (2018).
[60]W. Liu, F. Scheibel, T. Gottschall, E. Bykov, I. Dirba, K. Skokov, and O. Gutfleisch, Appl. Phys. Lett. **119**, 022408 (2021).
[61]A. Biswas, R. K. Chouhan, A. Thayer, Y. Mudryk, I. Z. Hlova, O. Dolotko, and V. K. Pecharsky, Phys. Rev. Mater. **6**, 114406 (2022).
[62]J. Liu, Y. Gong, Y. You, X. You, B. Huang, X. Miao, G. Xu, F. Xu, and E. Brück, Acta Mater. **174**, 450 (2019).

[63]S. Samanta, S. Chatterjee, S. Ghosh, and K. Mandal, Phys. Rev. Mater. **6**, 094411 (2022).
[64]L. M. Moreno-Ramírez, J. Y. Law, J. M. Borrego, A. Barcza, J. M. Greneche, and V. Franco, "First order phase transition in high-performance La(Fe,Mn,Si) 13H despite negligible hysteresis" (unpublished) (2022).
[65]J. Y. Law, Á Díaz-García, L. M. Moreno-Ramírez, and V. Franco, Acta Mater. **212**, 116931 (2021).
[66]J. Y. Law, L. M. Moreno-Ramírez, Á Díaz-García, A. Martín-Cid, S. Kobayashi, S. Kawaguchi, T. Nakamura, and V. Franco, J. Alloys Compd. **855**, 157424 (2021).
[67]T. Samanta, P. Lloveras, A. U. Saleheen, D. L. Lepkowski, E. Kramer, I. Dubenko, P. W. Adams, D. P. Young, M. Barrio, J. L. Tamarit, N. Ali, and S. Stadler, Appl. Phys. Lett. **112**, 021907 (2018).
[68]T. L. Phan, T. A. Ho, T. V. Manh, N. T. Dang, C. U. Jung, B. W. Lee, and T. D. Thanh, J. Appl. Phys. **118**, 143902 (2015).
[69]L. M. Moreno-Ramírez, C. Romero-Muñiz, J. Y. Law, V. Franco, A. Conde, I. A. Radulov, F. Maccari, K. P. Skokov, and O. Gutfleisch, Acta Mater. **175**, 406 (2019).
[70]L. M. Moreno-Ramírez, C. Romero-Muñiz, J. Y. Law, V. Franco, A. Conde, I. A. Radulov, F. Maccari, K. P. Skokov, and O. Gutfleisch, Acta Mater. **160**, 137 (2018).
[71]B. Kaeswurm, V. Franco, K. P. Skokov, and O. Gutfleisch, J. Magn. Magn. Mater. **406**, 259 (2016).
[72]J. Lai, A. Bolyachkin, N. Terada, S. Dieb, X. Tang, T. Ohkubo, H. Sepehri-Amin, and K. Hono, Acta Mater. **232**, 117942 (2022).
[73]J. H. Xu, W. Y. Yang, Q. H. Du, Y. H. Xia, H. L. Du, J. B. Yang, C. S. Wang, J. Z. Han, S. Q. Liu, Y. Zhang, and Y. C. Yang, J. Phys. D: Appl. Phys. **47**, 5 (2014).
[74]J. Y. Law, Á Díaz-García, L. M. Moreno-Ramírez, V. Franco, A. Conde, and A. K. Giri, Acta Mater. **166**, 459 (2019).
[75]J. V. Leitao, M. van der Haar, A. Lefering, and E. Bruck, J. Magn. Magn. Mater. **344**, 49 (2013).
[76]J. Lai, X. Tang, H. Sepehri-Amin, and K. Hono, Scr. Mater. **183**, 127 (2020).
[77]J. Q. Deng, Y. H. Zhuang, J. Q. Li, and K. W. Zhou, J. Alloys Compd. **428**, 28 (2007).
[78]X. Chen, Y. G. Chen, and Y. B. Tang, J. Alloys Compd. **509**, 9604 (2011).
[79]X. Hai, Ph.D. thesis, Grenoble Alpes University, 2016.
[80]Q. Zhou, Z. G. Zheng, Z. G. Qiu, Y. Hong, Y. Mozharivskyj, and D. C. Zeng, J. Supercond. Novel Magn. **32**, 3987 (2019).
[81]Y. Yuan, Y. Wu, X. Tong, H. Zhang, H. Wang, X. J. Liu, L. Ma, H. L. Suo, and Z. P. Lu, Acta Mater. **125**, 481 (2017).
[82]J. Huo, L. Huo, J. Li, H. Men, X. Wang, A. Inoue, C. Chang, J.-Q. Wang, and R.-W. Li, J. Appl. Phys. **117**, 073902 (2015).
[83]H. Yin, J. Law, Y. Huang, V. Franco, H. Shen, S. Jiang, Y. Bao, and J. Sun, Mater. Des. **206**, 109824 (2021).
[84]S. F. Lu, L. Ma, J. Wang, Y. S. Du, L. Li, J. T. Zhao, and G. H. Rao, J. Alloys Compd. **874**, 159918 (2021).
[85]S. F. Lu, L. Ma, G. H. Rao, J. Wang, Y. S. Du, L. Li, J. T. Zhao, X. C. Zhong, and Z. W. Liu, J. Mater. Sci.: Mater. Electron. **32**, 10919 (2021).
[86]C. M. Pang, C. C. Yuan, L. Chen, H. Xu, K. Guo, J. C. He, Y. Li, M. S. Wei, X. M. Wang, J. T. Huo, and B. L. Shen, J. Non-Cryst. Solids **549**, 120354 (2020).
[87]X. Miao, W. Wang, H. Liang, F. Qian, M. Cong, Y. Zhang, A. Muhammad, Z. Tian, and F. Xu, J. Mater. Sci. **55**, 6660 (2020).
[88]I. A. Radulov, K. P. Skokov, D. Y. Karpenkov, T. Braun, and O. Gutfleisch, IEEE Trans. Magn. **51**, 1 (2015).
[89]I. A. Radulov, K. P. Skokov, D. Y. Karpenkov, T. Gottschall, and O. Gutfleisch, J. Magn. Magn. Mater. **396**, 228 (2015).
[90]I. A. Radulov, D. Y. Karpenkov, K. P. Skokov, A. Y. Karpenkov, T. Braun, V. Brabaender, T. Gottschall, M. Pabst, B. Stoll, and O. Gutfleisch, Acta Mater. **127**, 389 (2017).
[91]I. A. Radulov, D. Y. Karpenkov, M. Specht, T. Braun, A. Y. Karpenkov, K. P. Skokov, and O. Gutfleisch, IEEE Trans. Magn. **53**, 1 (2017).
[92]T. Lei, K. Navickaitė, K. Engelbrecht, A. Barcza, H. Vieyra, K. K. Nielsen, and C. R. H. Bahl, Appl. Therm. Eng. **128**, 10 (2018).
[93]K. Navickaitė, H. N. Bez, T. Lei, A. Barcza, H. Vieyra, C. R. H. Bahl, and K. Engelbrecht, Int. J. Refrig. **86**, 322 (2018).
[94]J. Liang, M. Masche, K. Engelbrecht, K. K. Nielsen, H. A. Vieyra, A. Barcza, and C. R. H. Bahl, Appl. Therm. Eng. **197**, 117383 (2021).
[95]L. Pfeuffer, J. Lemke, N. Shayanfar, S. Riegg, D. Koch, A. Taubel, F. Scheibel, N. A. Kani, E. Adabifiroozjaei, L. Molina-Luna, K. P. Skokov, and O. Gutfleisch, Acta Mater. **221**, 117390 (2021).
[96]L. Wang, H. Xuan, S. Liu, T. Cao, Z. Xie, X. Liang, F. Chen, K. Zhang, L. Feng, P. Han, and Y. Wu, J. Alloys Compd. **846**, 156313 (2020).
[97]H. Li, X. Meng, and W. Cai, Mater. Sci. Eng., A **725**, 359 (2018).
[98]Z. Yang, D. Cong, Y. Yuan, Y. Wu, Z. Nie, R. Li, and Y. Wang, Mater. Res. Lett. **7**, 137 (2019).
[99]Á Díaz-García, J. Y. Law, A. Cota, A. Bellido-Correa, J. Ramírez-Rico, R. Schäfer, and V. Franco, Mater. Today Commun. **24**, 101049 (2020).
[100]Á Díaz-García, J. Y. Law, M. Felix, A. Guerrero, and V. Franco, Mater. Des. **219**, 110806 (2022).
[101]Á Díaz-García, J. Revuelta, L. M. Moreno-Ramírez, J. Y. Law, C. Mayer, and V. Franco, Compos. Commun. **35**, 101352 (2022).
[102]F. Scheibel, C. Lauhoff, S. Riegg, P. Krooß, E. Bruder, E. Adabifiroozjaei, L. Molina-Luna, S. Böhm, Y. I. Chumlyakov, T. Niendorf, and O. Gutfleisch, Adv. Eng. Mater. **24**, 2200069 (2022).
[103]V. Franco and A. Conde, Int. J. Refrig. **33**, 465 (2010).
[104]B. K. Banerjee, Phys. Lett. **12**, 16 (1964).
[105]C. M. Bonilla, J. Herrero-Albillos, F. Bartolome, L. M. Garcia, M. Parra-Borderias, and V. Franco, Phys. Rev. B **81**, 224424 (2010).
[106]J. Y. Law, V. Franco, L. M. Moreno-Ramirez, A. Conde, D. Y. Karpenkov, I. Radulov, K. P. Skokov, and O. Gutfleisch, Nat. Commun. **9**, 2680 (2018).
[107]C. P. Bean and D. S. Rodbell, Phys. Rev. **126**, 104 (1962).
[108]V. Franco, J. Y. Law, A. Conde, V. Brabander, D. Y. Karpenkov, I. Radulov, K. Skokov, and O. Gutfleisch, J. Phys. D: Appl. Phys. **50**, 414004 (2017).
[109]L. M. Moreno-Ramírez, J. Y. Law, S. S. Pramana, A. K. Giri, and V. Franco, Results Phys. **22**, 103933 (2021).
[110]J. Y. Law, V. Franco, A. Conde, S. J. Skinner, and S. S. Pramana, J. Alloys Compd. **777**, 1080 (2019).
[111]N. H. van Dijk, J. Magn. Magn. Mater. **529**, 167871 (2021).
[112]C. R. Pike, A. P. Roberts, and K. L. Verosub, J. Appl. Phys. **85**, 6660 (1999).
[113]V. Franco and B. Dodrill, *Magnetic Measurement Techniques for Materials Characterization* (Springer, Cham, 2021).
[114]C.-I. Dobrotă and A. Stancu, J. Appl. Phys. **113**, 043928 (2013).
[115]J. C. Martínez-García, M. Rivas, D. Lago-Cachón, and J. A. García, J. Phys. D: Appl. Phys. **47**, 015001 (2014).
[116]V. Franco, T. Gottschall, K. P. Skokov, and O. Gutfleisch, IEEE Magn. Lett. **7**, 1 (2016).
[117]V. Franco, J. Appl. Phys. **127**, 133902 (2020).
[118]Á Díaz-García, L. M. Moreno-Ramírez, J. Y. Law, F. Albertini, S. Frabbrici, and V. Franco, J. Alloys Compd. **867**, 159184 (2021).
[119]L. M. Moreno-Ramírez and V. Franco, Metals **10**, 1039 (2020).
[120]L. M. Moreno-Ramirez and V. Franco, "Evaluation of magnetocaloric performance by Temperature First Order Reversal Curves (TFORC) distributions" (unpublished) (2023).
[121]V. Franco, J. S. Blazquez, and A. Conde, Appl. Phys. Lett. **89**, 222512 (2006).
[122]Á Díaz-García, J. Y. Law, P. Gębara, and V. Franco, JOM **72**, 2845 (2020).
[123]Á Díaz-García, J. Y. Law, L. M. Moreno-Ramírez, A. K. Giri, and V. Franco, J. Alloys Compd. **871**, 159621 (2021).
[124]J. Schmidt, M. R. G. Marques, S. Botti, and M. A. L. Marques, npj Comput. Mater. **5**, 83 (2019).
[125]S. Sanvito, C. Oses, J. Xue, A. Tiwari, M. Zic, T. Archer, P. Tozman, M. Venkatesan, M. Coey, and S. Curtarolo, Sci. Adv. **3**, e1602241 (2017).
[126]P. B. D. Castro, K. Terashima, T. D. Yamamoto, Z. Hou, S. Iwasaki, R. Matsumoto, S. Adachi, Y. Saito, P. Song, H. Takeya, and Y. Takano, NPG Asia Mater. **12**, 35 (2020).

[127]J. D. Bocarsly, E. E. Levin, C. A. C. Garcia, K. Schwennicke, S. D. Wilson, and R. Seshadri, Chem. Mater. **29**, 1613 (2017).
[128]T. O. Owolabi, K. O. Akande, S. O. Olatunji, A. Alqahtani, and N. Aldhafferi, AIP Adv. **6**, 105009 (2016).
[129]B. Zhang, X.-Q. Zheng, T.-Y. Zhao, F.-X. Hu, J.-R. Sun, and B.-G. Shen, Chin. Phys. B **27**, 067503 (2018).
[130]D. Tu, J. Yan, Y. Xie, J. Li, S. Feng, M. Xia, J. Li, and A. P. Leung, J. Mater. Sci. Technol. **96**, 241 (2022).